6th China-Japan-Korea Joint Symposium on Optimization of Structural and Mechanical Systems
June 22–25, 2010, Kyoto, Japan

Aerodynamic Design Optimization of New Conceptual Civil Aircraft

Takuya Nara[1], Masahiro Kanazaki[2]

[1] Tokyo Metropolitan University Asahigaoka 6-6, Hino, Tokyo, Japan, nara-takuya@sd.tmu.ac.jp
[2] Tokyo Metropolitan University Asahigaoka 6-6, Hino, Tokyo, Japan, kana@sd.tmu.ac.jp

Abstract

Blended-Wing-Body (BWB) aircraft is expected to be next generation airliner. While many studies for BWB has been performed for a large scale aircraft, an aircraft which is for regional jet is also expected. Such aircraft would be small (about 100-300 seats). In the development of such aircraft, BWB should be also discussed because it has aerodynamic advantage compared with conventional aircrafts. Therefore, the aerodynamic design optimization for a small size BWB is required for conceptual design. In this study, an initial BWB which has 150 seats configuration is designed using genetic algorithm (GA). Because BWB's fuselage has similar geometry to a conventional airfoil, two types of airfoil optimizations are preformed to decide the fuselage and outboard wing section, separately. Unstructured Euler analysis is applied to evaluate the aerodynamic performance of BWB initial design.

Keywords: *Blended-Wing-Body, Genetic Algorithm, Computer Flow Dynamics, Aircraft*

1. Introduction

Blended-Wing-Body (BWB) aircraft (Fig. 1) has possibility to be a next generation aircraft, because of its highly aerodynamic sophisticated geometry which reduce interference drag. That configuration is very different from the conventional one. Its fuselage is blended to wing surface and its cross section also gain lift. Therefore, BWB has great advantage in aerodynamic performance compared with the conventional aircraft. Many institutes study on BWB for a large aircraft, but it is reported that approximately a half of new demand is 100-200 seats aircraft at 2028, because the air traffic demand has been changing from Hub-and-Spoke to Point-to-Point [2]. Thus a small type aircraft should be considered for the next generation.

There are several problems to consider small size BWB. One of the most remarkable problems is that the cabin height has to be about 2.0m. Thus, a small BWB has passenger cabin which height is not so high. The cross section of BWB's fuselage is also same as airfoil. It suggests that small size BWB has relative thick airfoil as shown in Fig. 2. Because a thick airfoil doesn't have good aerodynamic performance, the detail of the geometry include a curvature should be decided for its aerodynamic efficiency.

In this study, design optimization procedure is considered for initial layout. Airfoil geometries, which are the span wise cross section of the BWB geometry, are designed using genetic algorithm (GA) [3, 4] with computational fluid dynamics (CFD). Optimum airfoil parameters are selected and applied to the three dimension initial geometry. In three dimension modeling process, BWB's planform is defined with cubic curve and linear line. The inboard, fuselage, planform has to connect outboard wing smoothly. So, from fuselage center to outboard wing is interpolated by cubic curve. The outboard wing planform is similar to a conventional aircraft wing. Then, linear interpolation is conducted. BWB three- dimensional aerodynamic performance is analyzed by unstructured Euler flow solver [5, 6].

Figure 1. Blended-Wing-Body aircraft [1]

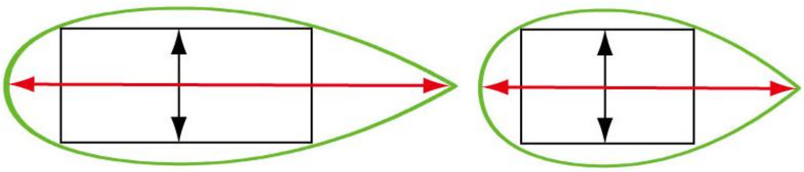

Figure 2. Cabin space in large and small fuselage cross sections

2. Cross Section Design of BWB

2.1. Geometry Definition Methods

2.1.1. Modified PARSEC Representation Method 1

In this study, the modified PARSEC representation methods developed by ourselves are applied. Thickness and camber line is defined by polynomial function Eqs. (1) and (2), respectively.

$$z_{\text{thickness}} = \sum_{n=1}^{5} a_n \times x^{\frac{2n-1}{2}} \tag{1}$$

$$z_{\text{camber}} = \sum_{n=1}^{5} b_n \times x^n \tag{2}$$

where a_n, b_n are decided by airfoil parameters shown in Fig. 3 and Fig. 4. Here, 10 design variables are defined as shown in Table 1.

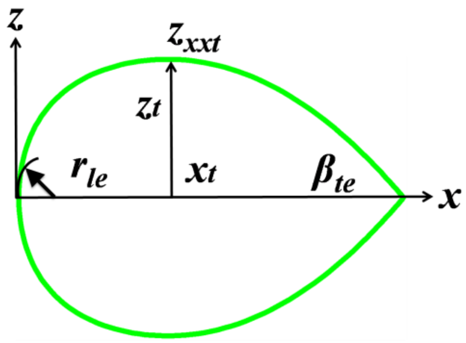

Figure 3. Definition of thickness distribution

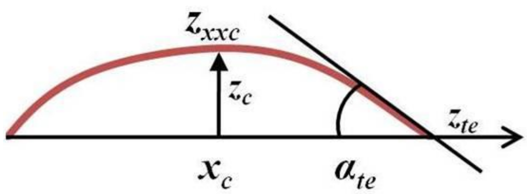

Figure 4. Definition of camber

Table 1. Modified PARSEC representation method 1 parameter name

Leading edge radius	Max thickness value	Max thickness value	Max thickness radius of curvature	Trailing edge expansion angle
r_{le}	x_t	z_t	z_{xxt}	β_{te}
Max camber location	Max camber value	Max camber radius of curvature	Camber trailing edge angle	Camber trailing edge z value
x_c	z_c	z_{xxc}	α_{te}	z_{te}

2.1.2. Modified PARSEC Representation Method 2

In modified PARSEC representation method 2, thickness distribution is decided by Eq. (1), but square root term added to camber's representation expressed as Eq. (3). By introduction of this term, the leading edge will be able to be improved as shown in Fig. 5.

$$z_{\text{camber}} = b_0 \times \sqrt{x} + \sum_{n=1}^{5} b_n \times x^n \tag{3}$$

where b_n are airfoil camber parameters. To decide every b_n, design variables are defined as shown in Fig. 6 and Table 2.

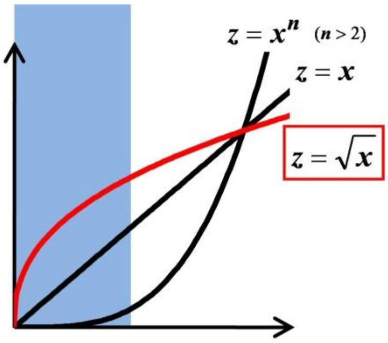

Figure 5. Influence of $\sqrt{X}$ in the geometry definition

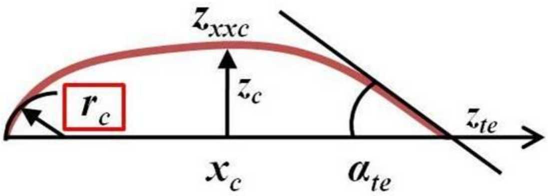

Figure 6. Definition of camber

Table 2. Modified PARSEC representation method 2 parameter name

Camber leading edge radius	Max camber location	Max camber value	Max camber radius of curvature	Camber trailing edge angle	Camber trailing edge z value
r_c	x_c	z_c	z_{xxc}	α_{te}	z_{te}

2.2. Design Variables

2.2.1. Design Variables for fuselage with Modified PARSEC Representation Method 1

Using Eq. (2), the camber around the leading edge is defined as relative small. The fuselage cross section's leading edge should be cockpit, thus this method 1 is applied to the definition of the fuselage cross section. The cross section of the proposed BWB fuselage has to be reflexed airfoil for aircraft trim balance. To define reflex camber line, the trailing edge gradient α_{te} has to be negative variables(Fig. 7). The fuselage cross section should have sufficient thickness to maintain the cabin volume. Design range of airfoil thickness is 10-30 %. Then, modified PARSEC representation method 1 parameters' ranges are defined as Table 3.

Figure 7. Airfoil with reflex camber

Table 3. Design space for fuselage definition

Thickness parameters	Min value	Max value	Camber parameters	Min value	Max value
r_{le}	0.005	0.06	x_c	0.1	0.5
x_t	0.3	0.6	z_c	0	0.05
z_t	0.05	0.15	z_{xxc}	-1	0
z_{xxt}	-1	0	α_{te}	-10	0
β_{te}	4	15	z_{te}	0	0.08

2.2.2. Design Variables for outboard wing with Modified PARSEC Representation Method 2

The airfoil of the outboard wing is defined modified PARSEC representation method 2. BWB outboard wing has similar thickness distribution and camber line to the conventional aircraft wing. Therefore, same parameter range is applied to this design. Thus, design space for the BWB's outboard airfoil is defined in Table. 4.

Table 4. Design space for outboard airfoil

Thickness parameters	Min value	Max value	Camber parameters	Min value	Max value
r_{le}	0.005	0.04	r_c	0	0.002
x_t	0.4	0.5	x_c	0.2	0.6
z_t	0.04	0.08	z_c	0	0.05
z_{xxt}	-1	-0.4	z_{xxc}	-0.03	0
β_{te}	4.2	6.4	α_{te}	3	8
-	-	-	z_{te}	-0.02	0.01

3. Airfoil Evaluation

Aerodynamic performances of airfoils are evaluated Navier-Stokes flow solver expressed as eq. (4).

$$\frac{\partial}{\partial t}\int_{\Omega} \Phi \, dv + \oint_{\partial\Omega} F \cdot d\vec{s} = 0 \tag{4}$$

where Φ is conserved quantity in volume. F is sum of conserved quantity which go in and out. Turbulent model is Baldwin-Lomax model. Space discretization is 191×91 C type structured grid as shown in Fig. 8. This grid is created algebraic method automatically [7]. Lower-upper Symmetric Gauss-Seidel (LU-SGS) implicit method is applied to time integration. Flux is evaluated by third order accurate upwind-discretization by MUSCL method [8, 9].

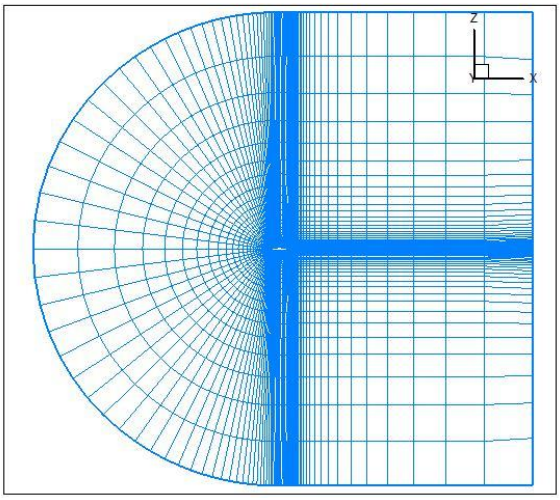

Figure 8. (a) Computational grid

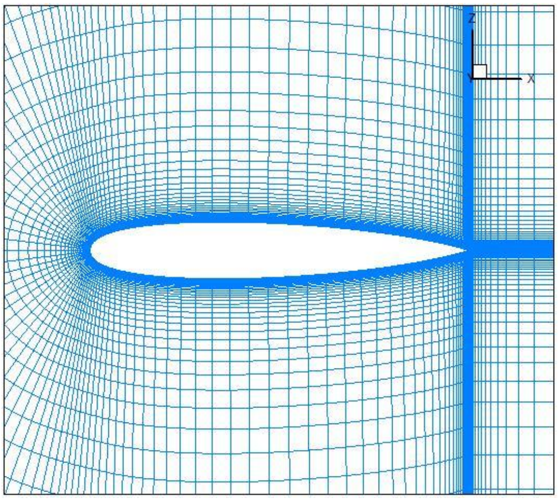

Figure 8. (b) Airfoil grid view

4. Optimization Method

To optimize the BWB's cross section, ARDRMOGA(Adaptive Range Divided Range Multi-Objective Genetic Algorithm) is applied [10, 11]. The design problem is defined as the maximization of the lift to drag ratio and the airfoil thickness at the same time. Genetic algorithm (GA) is inspired by the evolution of living organisms with regard to adaptation to the environment and the passing on of genetic information to the next generation (Fig. 9 (a)). GA is capable of finding a global optimum because they do not use function gradients, which often leads to local optimum. Thus, GA is a robust and effective method to handle highly non-linear optimization problems involving non-differentiable objective functions.

For divided range algorithm, cellular model is used. The cellular model DRMOGA is illustrated in Fig. 9 (b). This model divides the population according to sorting by solution or design space, which is reminiscent of *cells*. It includes a similar concept regarding migration. This model is characterized by the neighborhood searching to produce better solutions from non-dominated solutions. It means that the cellular model can prevent the crossover between the scattered parents in the solution space and it can search non-dominated solutions efficiently. To improve the design space automatically, adaptive range MOGA (ARMOGA) is applied in each cell.

In this study, redivision interval is set to 8, adaptive range interval is set to 6, sub-population number is set to 2, sub-population size is set to 10 and 20 and total generation number is set to 12 and 20 for fuselage and outboard wing cross section, respectively. General airliner wing cross section flow condition is assumed. Angle of attack is set on two degree and Mach number is 0.80. Reynolds number is 1.0×10^{7}.

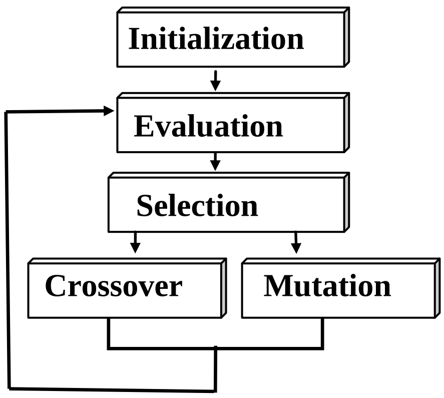

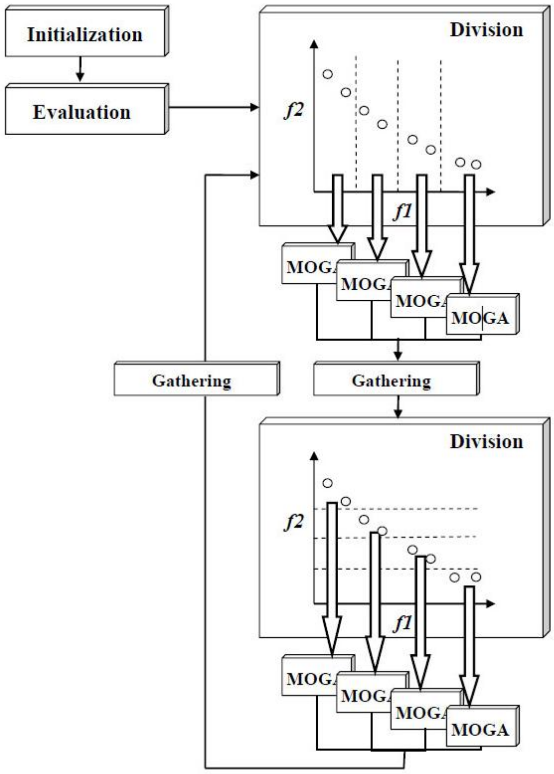

(a) Genetic algorithm (b) DRMOGA

Figure 9. Genetic algorithms applied in this design process; (a)Basis of GA, and (b)Procedure of DRMOGA.

3. Decision of Aircraft's Cross Sections

3.1 Fuselage

Fig. 10 illustrates non-dominated solutions between *l/d* vs. thickness ratio. Proposed BWB has a fuselage which the length is 25.0 m, and the cabin height is 2.0 m and the height for structure is 1.0 m. Thus, required thickness becomes 12% chord length. From Fig. 10, Fuselage-1, 2, 3 and 4 are compared. Fuselage-1, 2 each design achieves good *l/d*, but their thickness is 10.4% and 11.8%, respectively. Therefore, they can't compose a cabin and structure. Fuselage-3 has moderate l/d among non-dominated solutions and it also has enough maximum thickness (about 12.5%). However Fuselage-3 can't compose the cabin box. Fuselage-4 has minimum *l/d* among Fuselage-1, 2, 3, and 4, but it has enough thickness. Fig. 11 illustrates Fuselage-4 pressure distribution. It indicates the airfoil gets reverse lift at the aft position. Negative lift at the airfoil aft position is an advantage to trim the aircraft. Thus, Fuselage-4 is suitable for a fuselage cross section.

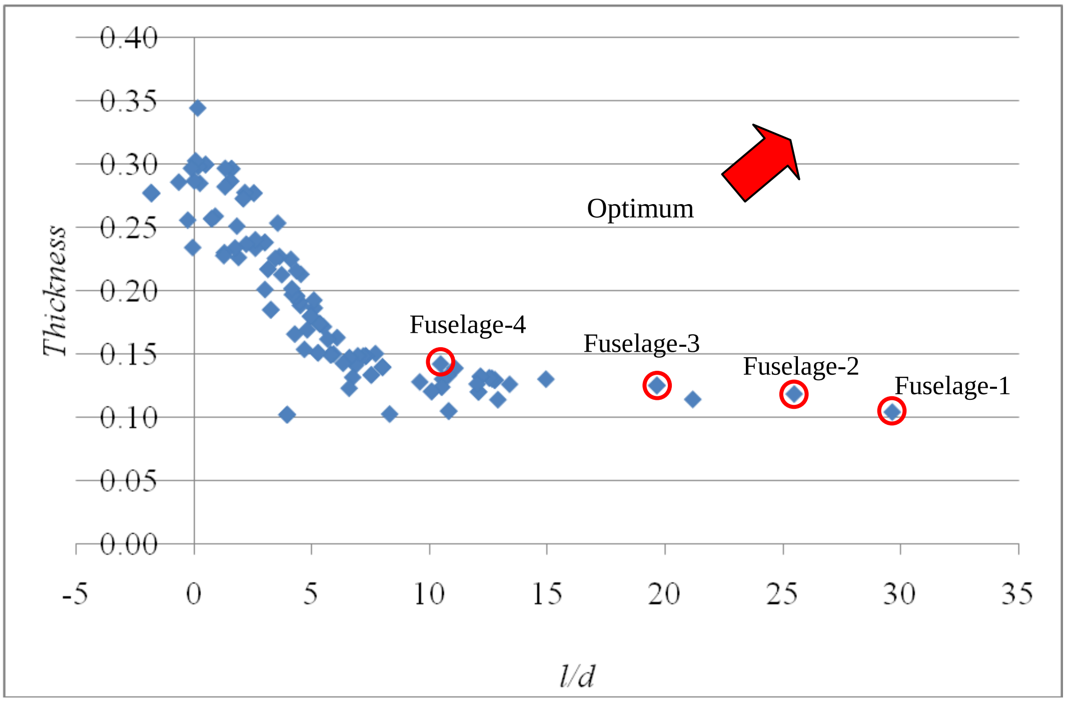

Figure 10. Fuselage section airfoil solution l/d-thickness ratio

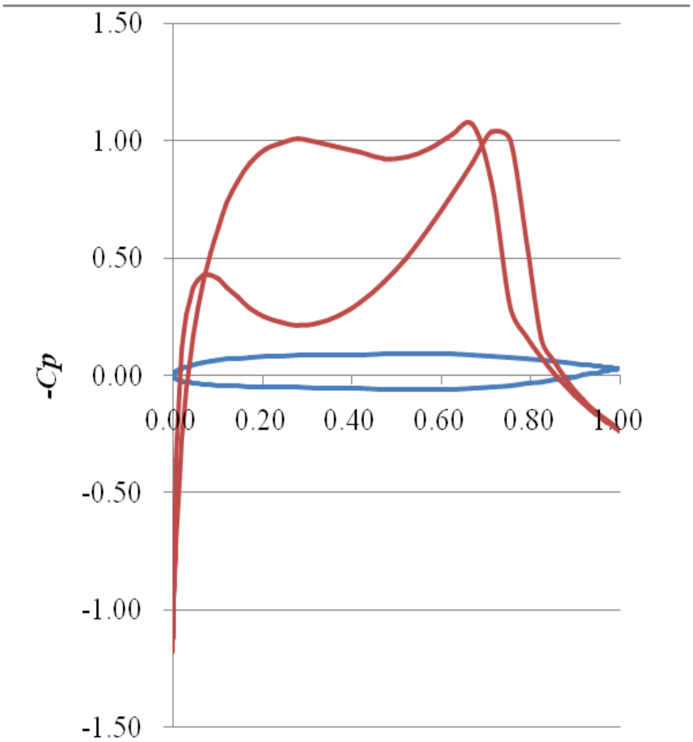

Figure 11. Fuselage-5 pressure distribution

3.2 Outboard Wing

Fig. 12 shows the non-dominated solutions between *l/d* vs. thickness. In this figure, Out-Design achieves maximum *l/d* (67.6). While shock wave appeared on the airfoil around 55% chord length, thickness is relative small (9.4%), so the airfoil drag becomes little. Thus, it achieves the highest *l/d*. In this study, this geometry is used for the outboard wing of the initial geometry of the proposed BWB.

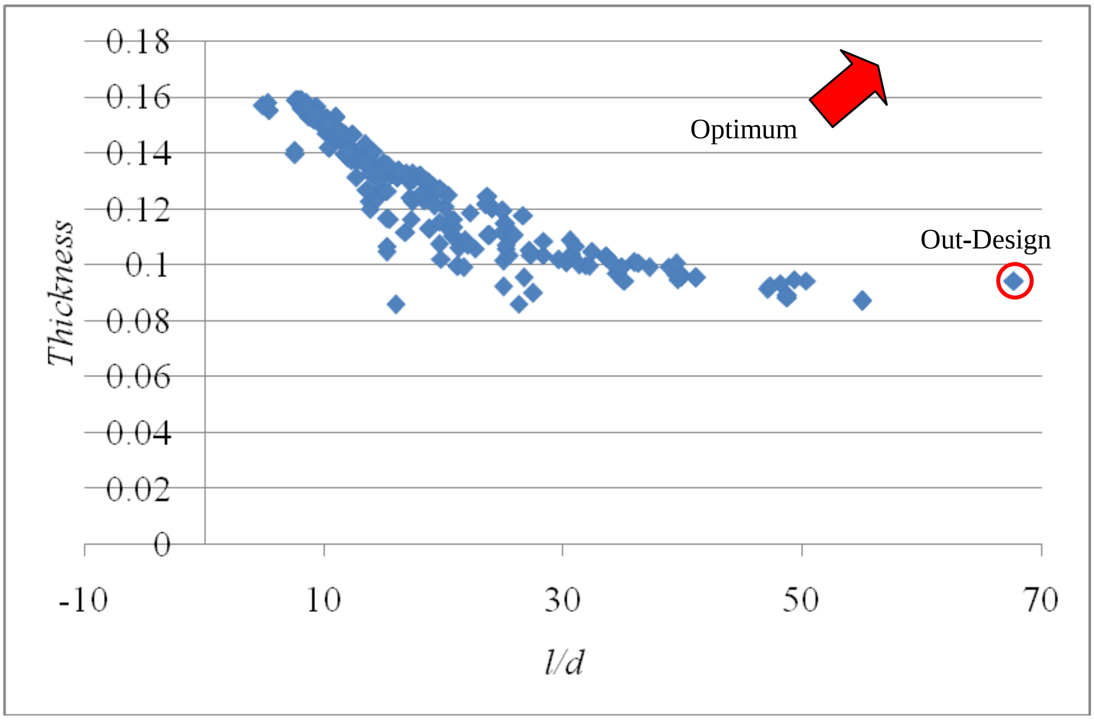

Figure 12. Outer wing section solution l/d-thickness ratio

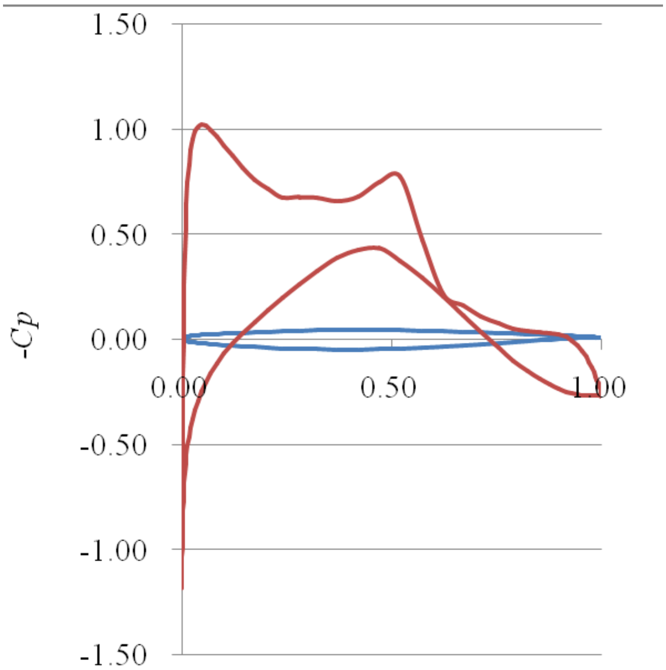

Figure 13. Out-1 flow condition

4. Three-dimension Evaluation

4.1 Initial Geometry

Fig. 14 illustrates the definition of the BWB's planform. Three cross sections which defined for BWB geometry discussed in Section 3. Here, at the cross section of the fuselage center is designed in 3.1.

The cross section between the fuselage and the outboard wing, and the wing tip are designed in 3.2. The three dimensional geometry of outboard wing (the connection between the fuselage and the wing to wing tip) is linearly interpolated. The three dimensional geometry between the fuselage and the wing is interpolated by a cubic curve. At the fuselage center, the curve is vertical to the aircraft center line. And C1 continuous condition is considered to connect the inboard wing and the outboard wing.

Fig. 15 illustrates planform parameter. Inboard and outboard wing has three parameters respectively. To define the inboard wing planform there are three parameter the connect airfoil span and front position, scale relative to root airfoil. Outboard wing has three design variables, which are sweep back, taper ratio and aspect ratio. The parameters for initial planform are shown in Table 5. Here, the planform parameters of the BWB developed by NASA [1] are followed. And checked that the cabin is composed by the surface.

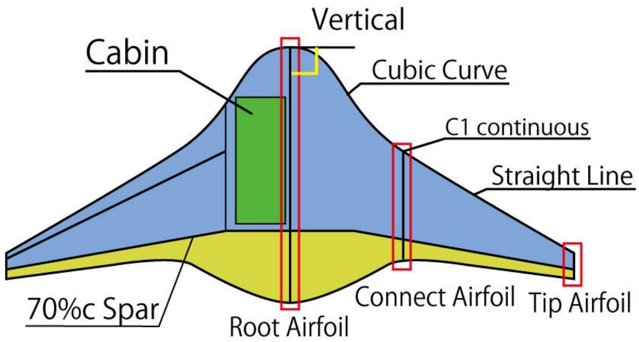

Figure 14. Planform definition

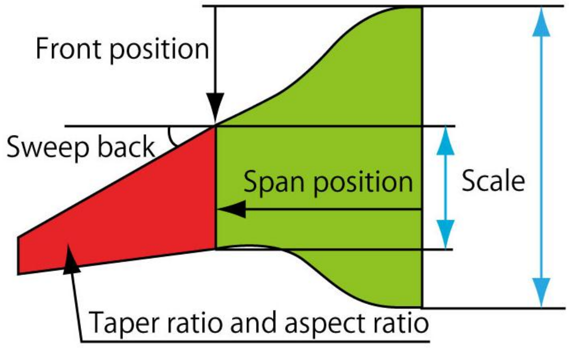

Figure 15. Parameters for BWB's planform

Table 5. Initial planform parameter

Parameter	Connect airfoil			Outboard wing		
	Front position (-)	Scale (relative to root airfoil)	Span position (-)	Sweep (degree)	Taper ratio (-)	Aspect ratio (-)
	0.64	0.20	0.50	30.0	0.35	2.50

4.2 Aerodynamic Evaluation

Aerodynamic performance of BWB is evaluated using TAS code (Tohoku university Aerodynamic Simulation code)[5, 6], an unstructured grid flow solver. Computational mesh is generated by Mixed-Element Grid Generator in 3 Dimensions (MEGG3D)[12, 13] as shown in Fig. 16. Compressive Euler equation is solved while angles of attack are changed. Free stream Mach number is set on 0.80.

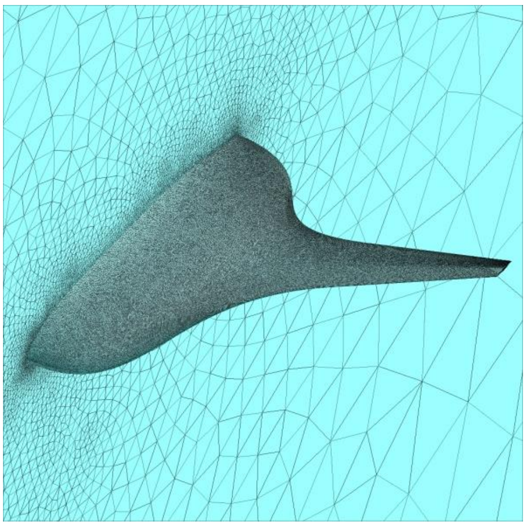
Figure 16. Computational grid

4.3 Result

Figure17 shows angle of attack *vs*. C_L, and Fig.18 shows angle of attack *vs*. C_D, Fig. 19 shows angle of attack *vs*. *L/D*. According to Fig. 19, this aircraft has maximum *L/D* at angle of attack of four degrees. Figure20 illustrates the Mach number contour and the stream line at angle of attack of four degrees. From this picture, the span-wise flow from the fuselage to the outboard wing can be observed. Additionally, two compressive points as shown by dotted line is also observed. In a transonic wing, only one compressive area conventionally appears, that is local shock wave. Designed airfoils discussed in section three also have one local shock around half cord length. This result suggests that such two compressive point appear by three dimensional effect which means the aerodynamic interaction between thick fuselage and outboard wing. This interaction also affects the aerodynamic phenomena on the outboard wing. Therefore, the final aircraft geometry should be proposed by the three dimensional optimization in consideration of the interaction between the fuselage and the outboard wing.

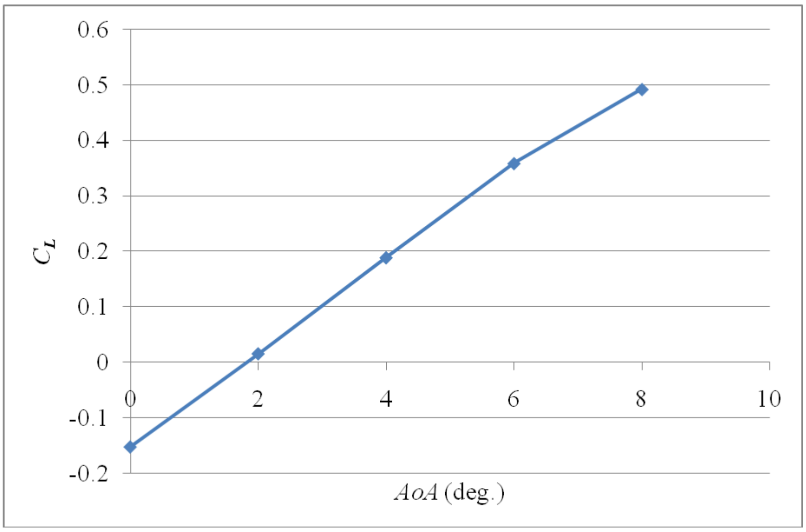

Figure 17. Initial BWB C_L-*AoA*

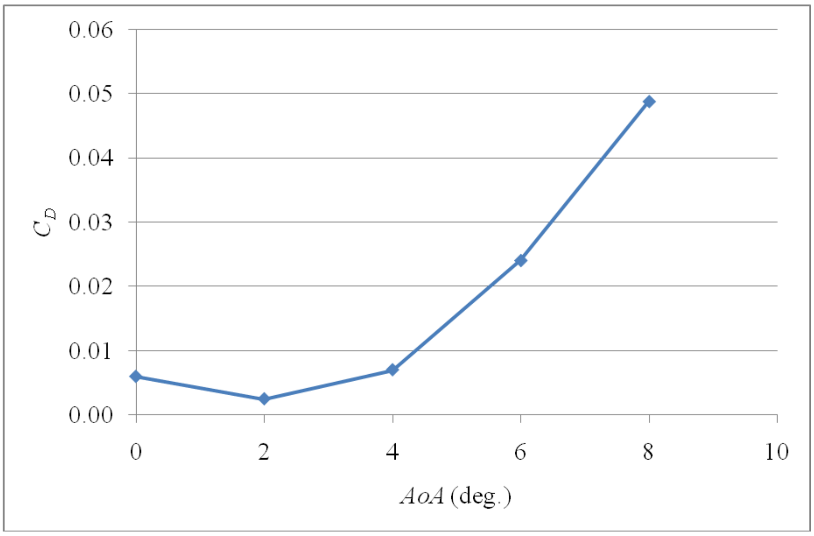

Figure 18. Initial BWB C_D-*AoA*

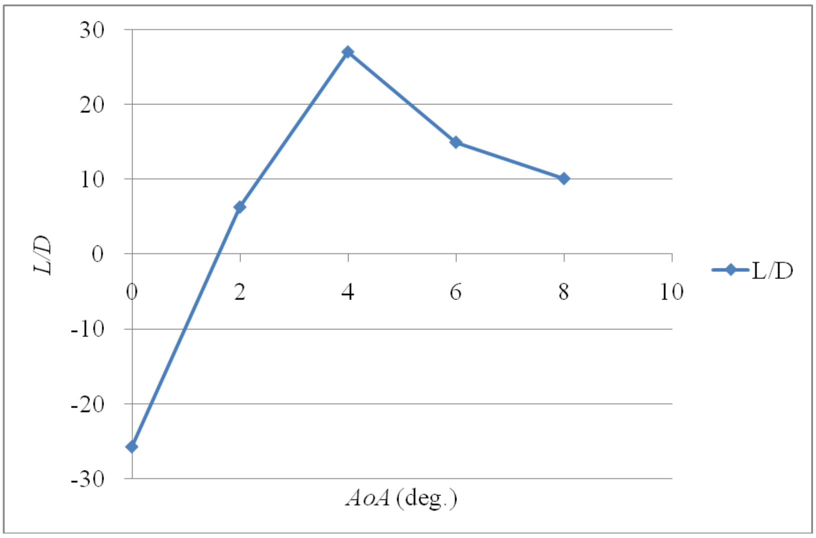

Figure 19. Initial BWB *AoA*-*L/D*

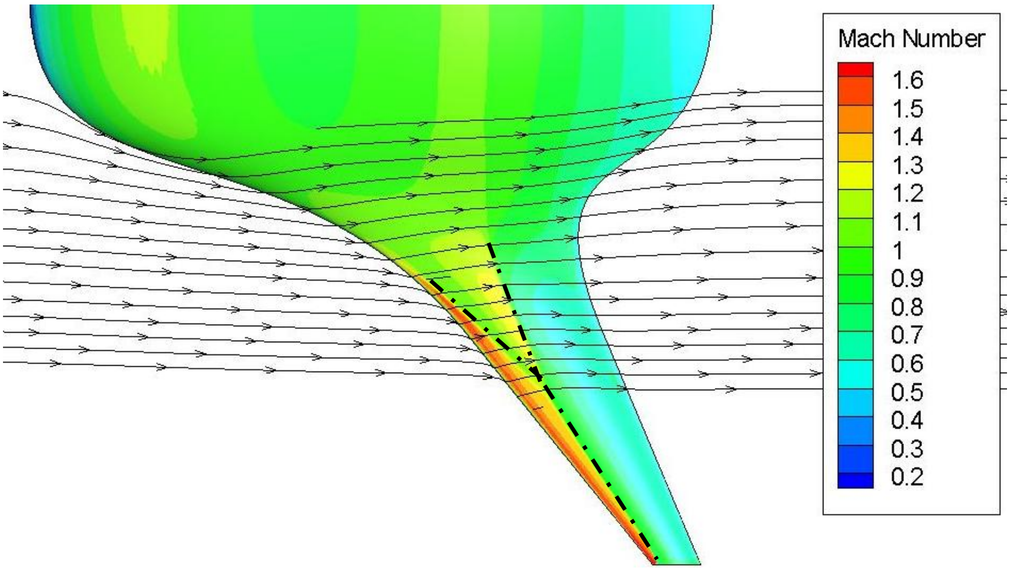

Figure 20. Mach number contour and stream line at angle of attack 4 deg.

5. Conclusion

In this study, the conceptual design and the aerodynamic design optimization is performed to propose the initial geometry of the blended-wing-body as a small size aircraft. Airfoils at the fuselage and the outboard wing are separately designed by MOGA. In MOGA process, the distributed scheme is employed with the range adaptation algorithm. Every individual's aerodynamic performances are evaluated using Navier-Stockes solver. Non-dominated solutions are obtained and airfoil designs are selected for the fuselage section and the outboard wing section. For the fuselage, a reflex camber airfoil is selected because the fuselage has to gain the negative lift around the trailing edge to maintain the trim balance. For the outboard wing, the design which achieves maximum L/D among the non-dominated solutions is selected. It was similar to conventional transonic airfoil. As their result, three dimensional geometry could be designed using these airfoils and its aerodynamic performance is also investigated using unstructured Euler solver. This result suggests that the shock wave interaction is severe problem in the design of the small size BWB.

Reference

[1] http://www.dfrc.nasa.gov/ (last accessed on 29th, August, 2009).
[2] N. Baba, Market forecast for commercial airplanes, Proceedings of the Wind Tunnel Technology Association 74th Meeting, pp. 9-11, 2006.
[3] D. E. Goldberg, Genetic algorithms in search, optimization & Machine learning, Addison-Wesley Publishing Company, Inc., 1989.
[4] J. E. Rawlins Gregory, Foundations of genetic algorithms, Morgan Kaufmann Publishers, Vol. 1-4, 1991.
[5] S. Obayashi and G. P. Guruswany, Convergence acceleration of an aeroelastic Navier-Stokes Solver, AIAA J., Vol. 33, pp. 157-159, 1998.
[6] D. Sharov and K. Nakahashi, Hybrid prismatic/tetrahedral grid generation fore viscous flow applications AIAA J., Vol. 36, pp. 157-159, 1998.
[7] L. E. Eriksson, Generation of boundary-conforming grids around wing-body configurations using transfinite interpolation, AIAA Journal, Vol. 20, pp. 1313-1320, 1982.
[8] B. van Leer, Toward the ultimate conservative difference scheme. 4 a new approach to numerical convection, Journal of Computational Physics, Vol. 23, 276-299, 1977.
[9] B. van Leer, Toward the ultimate conservative difference scheme. 5 a second-order sequel to Godunov's method, Journal of Computational Physics, Vol. 32, 101-136, 1979.
[10] D. Sasaki and S. Obayashi, Efficient search for trade-offs by adaptive range multi-objective genetic algorithms, AIAA Journal of Aerospace Computing, Information and Communication, pp. 44-64, 2005.
[11] T. Hiroyasu and M. Miki and S. Watanabe, The new model of parallel genetic algorithm in multi-objective optimization problems (divided range multi-objective genetic algorithm), IEEE Proceedings of the Congress on Evolutionary Computation 2000, Vol. 1, pp. 333-340, 2000.
[12] Y. Ito and K. Nakahashi, Direct surface triangulation using stereolithography data, AIAA Journal, Vol. 40, pp. 490-496, 2002.
[13] Y. Ito and K. Nakahashi, Surface triangulation for polygonal models based on CAD data, International Journal for Numerical Methods in Fluids, Vol. 39, pp. 75-96, 2002.